

The Development of New Nanoplatfoms Based on Albumin and Graphene Oxide for Aticancer Therapy

ELENA IULIANA BIRU¹, ANDREI SARBU², HORIA IOVU^{1,3*}

¹Advanced Polymer Materials Group, National University of Science and Technology Politehnica Bucharest, 1-7 Gheorghe Polizu Str., 011061 Bucharest, Romania

²National Institute for Research & Development in Chemistry and Petrochemistry ICECHIM, Advanced Polymer Materials and Polymer Recycling Group, 202 Splaiul Independentei, 060021, Bucharest, Romania

³Academy of Romanian Scientists, 54 Splaiul Independentei, 050085, Bucharest, Romania

Abstract: *This study focuses on the covalent functionalization of the carboxylated graphene oxide layers with human serum albumin for developing new nanoplatfoms capable of efficient drug loading and release for antitumor therapy. Thus, new GO-HSA conjugates have been developed and their interactions with methotrexate (MTX) molecules were evidenced through FT-IR, UV-Vis and Raman spectroscopy. The cumulative in vitro release profiles of MTX drug from GO-HSA-MTX nanoplatfoms were analyzed through UV-Vis spectroscopy showing a more controlled release behavior of MTX drug under acidic conditions that simulate the tumor microenvironment demonstrating the potential use of GO-HSA-MTX as antitumoral nanocarriers.*

Keywords: *albumin, drug release, methotrexate*

1. Introduction

Although significant advances have been made in developing new targeted and effective therapies, cancer remains one of the most common causes of death in the world. Drug treatments are nowadays the most used approaches to eliminate the fast-growing tumorous cells from the body and thus, the development of smart, effective, and targeted drug delivery nanocarriers is a major concern in medical science. The injection administration of the drugs is considered to be a faster method for reaching the targeted tumorous site, but they have to be perfused in high and possible toxic dosage [1]. The oral route is many times preferred since in most cases shows increased safety and is convenient for the patients. However, there is still an overwhelming need for mechanically stable nanocarriers to encapsulate therapeutic agents in order to avoid burst release and clearance from the body.

Currently, both natural and synthetic biodegradable polymers have attracted much interest as favorable therapeutic delivery systems due to excellent biocompatibility, lack of toxicity and immunogenic response and ease in tailoring suitable composition for controlling drug loading, time, and place of *in vivo* release [2]. Among natural polymers, proteins have been distinguished for their vital role in biological processes and their ability for specific drug delivery [3]. In comparison with synthetic polymers, many natural proteins are water-soluble, highly biocompatible, and inexpensive, therefore preferred for various biomedical applications including hydrogels for tissue engineering [4, 5], gene therapy for genetic diseases treatment [6] and nanoparticles for anticancer therapy [7]. Moreover, their pharmacokinetic behavior, degradation profile and mucoadhesive nature proved to be very appealing for developing drug delivery nanocarriers for different types of cancers such as breast [8], skin [9] and prostate [10]. Human serum albumin (HSA) is one of the most abundant protein found in human blood being synthesized in the liver hepatocytes and produced and released daily to the vascular system [11]. Having a molecular weight of approximately 66 kDa [12], albumin contains numerous cysteine amino-acidic residues that establish disulfide bridges contributing to the stability of the structure. Recently, albumins drug delivery systems based on carbon nanomaterials have attracted very much interest due to their ability to create drug reservoirs for enhancing drug biodistribution and bioavailability [13].

*email: horia.iovu@upb.ro

Carbon nanomaterials represent extremely interesting nanoplatforms for protein immobilization as they exhibit high surface area, low toxicity after proper functionalization and acceptable biocompatibility [14]. Nowadays, graphene derivatives are extensively studied as potential candidates for advanced biomedical applications such as smart drug delivery [15], gene therapy [16], anticancer treatments [17], controlled and stimuli-responsive drug delivery [18], theranostics [19], antibacterial [20] and antitumoral [21] phototherapies. Graphene oxide (GO) is obtained by chemical oxidation of graphite in the presence of strong oxidizing agents and ultrasonic cleavage, at the end presenting on its surface a significant number of reactive groups such as hydroxyl, carboxyl and epoxy that can be conveniently submitted to further functionalization and protein binding [22]. In this study, we propose the development of new nanoplatforms with complex structures capable of immobilizing the HSA structure onto the GO surface and methotrexate as anticancer drug with improved thermo-stability and controlled drug release.

2. Materials and methods

2.1. Materials

Carboxylated graphene (GO-COOH) containing 0.7 mmol of GOOH/g was purchased from NanoInnova Technologies (Madrid, Spain) and used as received. Human Serum Albumin (HSA) (lyophilized powder, $\geq 96\%$) and N-(3Dimethylaminopropyl)-N'-ethyl carbodiimide hydrochloride (EDC), sodium phosphate dibasic (Na_2HPO_4) 98%, potassium phosphate monobasic (KH_2PO_4) 98% and methotrexate (MTX) $\geq 98\%$ were purchased from Sigma Aldrich (Germany) and have been used without any purification.

2.2. Preparation of graphene oxide nanoplatforms loaded with HSA and MTX

Fifty milligrams of GO-COOH were dispersed in 50 mL of distilled water. The obtained suspension was further submitted to ultrasonication for one hour on ice bath to ensure a better dispersion of the GO layers. To create the covalent attachment of the HSA protein onto the graphene layers (Figure 1), the carboxyl groups (-COOH) from the surface of GO were activated using the EDC coupling agent. Thus 5 mg of EDC were added to GO-COOH suspension and further sonicated for 30 min then 25 mg of HSA protein were added under constant stirring for 24 h at room temperature. Subsequently, 5 mg methotrexate were added dropwise and left to stir for one hour and the color of the suspension became slightly green. The suspension was filtered, and in the end the obtained precipitate was cleansed with distilled water and dried at room temperature.

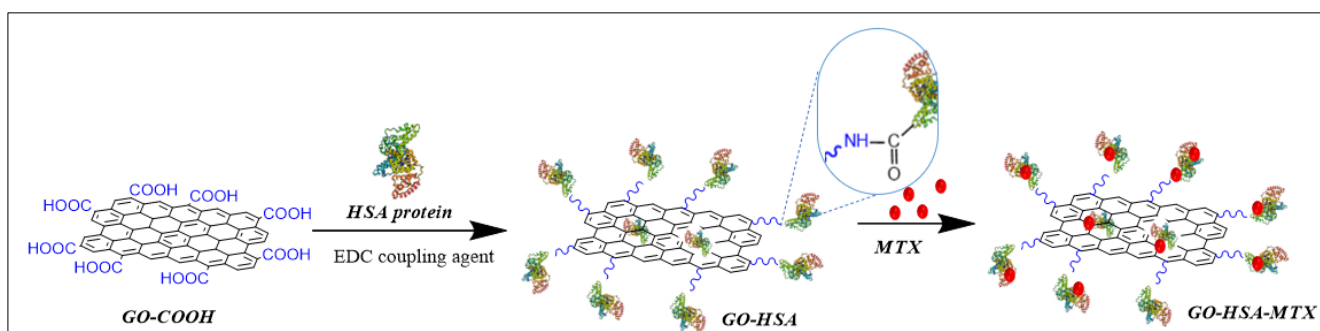


Figure 1. The synthesis route for the graphene oxide nanoplatforms loaded with HSA protein and MTX drug

2.3. Instruments

The FT-IR spectra were recorded on a Bruker instrument. Total reflection attenuation (ATR) module at 4 cm^{-1} resolution and $600\text{--}4000\text{ cm}^{-1}$ range was used and the final spectra are the average of 32 scans.

The Raman curves were recorded with a Renishaw Raman microscope with 10x objective using the laser wavelength of 785 nm and a laser power of 14 mW. Raman spectra were collected in the range $200\text{--}3400\text{ cm}^{-1}$.

Thermogravimetric analyses (TGA) were performed on a TG 209 F1 Libra instrument (NETZSCH-Gerätebau GmbH, Selb, Germany) as follows: a sample amount (~5 mg) was submitted to heating with a heating rate of 10°C/min in the temperature range 20-600°C. The analyses were performed in nitrogen atmosphere, the gas flow in the furnace being 20 mL/min using a Platinum/Rhodium crucible.

2.4. Encapsulation efficiency (EE) of the MTX and the drug release study

Both the encapsulation efficiency of MTX and the drug release behavior were determined by UV-VIS spectrometry and the results were recorded on a UV-VIS NIR Spectrometer (UV-3600) on a 1 cm quartz cell, at room temperature in the range of 200-500 nm wavelengths. The EE was determined using the following equation:

$$EE (\%) = ((M_{i\text{ MTX}} - M_{f\text{ MTX}})/M_{i\text{ MTX}}) \times 100,$$

where $M_{i\text{ MTX}}$ is the initial amount of MTX drug and $M_{f\text{ MTX}}$ represents the amount of unloaded drug amount. The EE was calculated as approximately 34%.

The dialysis method was used to determine the release profile of the MTX drug from the modified nanomaterials. Thus, 1 mL of GO-HSA-MTX suspension was placed in a dialysis sack (1000 Da MWCO), and dialysis was performed in PBS both at pH 7.4 (simulating the normal physiological conditions) and at pH 5.3 (mimicking the acidic pH in the tumor cell environment) at 37°C with shaking moderate (150 rpm). At predetermined time intervals, 1 mL of release medium was removed for analysis and an equivalent volume of release medium was filled into the dialysis vessel. The cumulative amount of MTX released was determined by UV-Vis absorption spectroscopy using the following equation:

$$\text{Cumulative drug release (\%)} = (M_t/M_{\text{initial}}) \times 100,$$

where M_t is the amount of the released drug from GO-HSA-MTX at time t and M_{initial} refers to the initial amount of drug introduced on the GO-HSA nanoplateforms.

3. Results and discussions

Human serum albumin (HSA) was covalently attached to the carboxylated graphene oxide (GO-COOH) surface through amide interactions in the presence of EDC forming GO-HSA nanostructures which were subsequently loaded with MTX drug for chemotherapeutic activity. The successful conjugation of HSA to GO-COOH surface and MTX loading, and their interactions have been firstly confirmed by Fourier Transformed Infrared (FT-IR) spectrometry and the results are shown in Figure 2. The FT-IR spectrum of the raw material GO-COOH shows the characteristic signals ascribed to the C=O (1725 cm⁻¹) and C-O vibrations (1046 cm⁻¹) from the carboxyl functionalities. Furthermore, the presence of C=C vibrations from the planar structure of graphene layers are observed at 1585 cm⁻¹. In the case of HSA protein, the FT-IR spectrum presents an important signal at 1650 cm⁻¹ representing the amid I from the protein structure attributed to the -NH-C=O stretch vibrations of the peptide linkages [23]. The signals around 2930 cm⁻¹ are attributed to the methyl and methylene groups found in the primary structure of HSA. Moreover, the signals from 1240 cm⁻¹ and 1086 are assigned to the vibrations of anti-symmetric and symmetric C-O stretching from the protein structure. After the covalent functionalization of GO-COOH with HSA and the therapeutic drug MTX, the FT-IR spectrum of the final product proved the successful attachment of the HSA protein onto GO-COOH surface and MTX loading. The introduction of HSA and MTX leads to the presence of a broader absorption band in the range of 3300 – 3400 cm⁻¹ characteristic to the multiple -NH- vibrations found both in the HSA and MTX structure. Furthermore, the presence of HSA protein covalently attached to GO-COOH was confirmed by the presence of the -NH-C=O stretch vibrations of the peptide linkages at 1630 and 1516 cm⁻¹. The MTX conjugation onto GO-HSA nanoplateforms was further noticed by the presence of the characteristic signals assigned to the asymmetric and symmetric -CH₃ bending vibrations (1016 cm⁻¹) and C=O

vibration found at 1148 cm^{-1} [24].

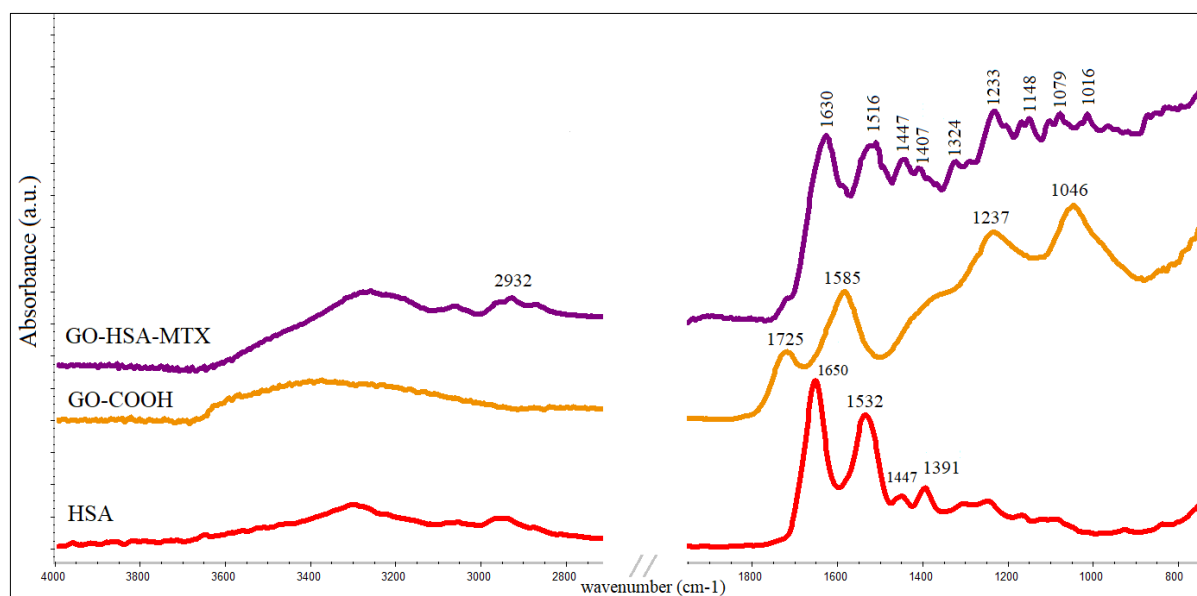


Figure 2. The FT-IR spectra of HSA protein, carboxylated graphene oxide and graphene oxide nanoplateforms loaded with HSA and MTX drug

Furthermore, the Raman spectrometry was employed as a useful method for analyzing structural modifications in graphene derivatives because it monitors the D band ($\sim 1360\text{ cm}^{-1}$) and the G band ($\sim 1595\text{ cm}^{-1}$) as observed in Figure 3. The D-mode vibration is caused by the disordered or defects found in the structure of the graphene layers. The G band is generated by C-C bond stretching vibrations generally found in graphitic materials and is characteristic to all sp^2 hybridized carbonaceous materials [25]. In the case of GO-HSA-MTX nanoplateforms, it is observed that the ratio of D signal intensity to G signal intensity (ID/IG) is higher, which demonstrates the adsorption of MTX drug on the GO-COOH surface and the presence of strong interactions between graphene and protein planes. In addition, the incorporation of GO-COOH layers into the protein matrix leads to a better exfoliation of the graphene layers, as suggested by the presence of 2D and G' signals characteristic of a reduced number of GO-COOH layers.

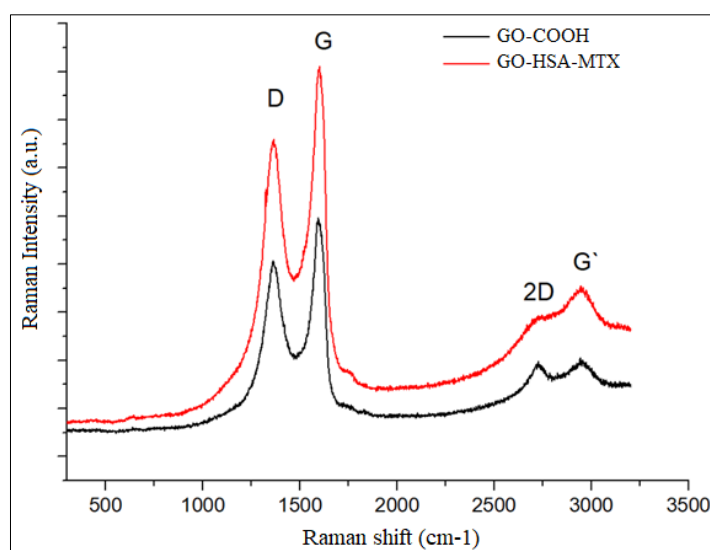


Figure 3. The Raman spectra of GO-COOH and GO-HSA-MTX

The developed nanoplatforms were also characterized through UV-Vis spectroscopy. As presented in Figure 4, the UV-Vis spectrum of the MTX drug shows strong π - π^* interactions at 258, 304 and 372 nm wavelengths due to the presence of heteroatomic pterine chromophore [26]. In the case of HSA protein, the UV-Vis spectrum presents only one absorption peak at 279 nm which is assigned to the presence of aromatic amino acids from the protein structure such as tryptophan, tyrosine, and phenylalanine [27, 28]. The UV-Vis spectrum of GO-HSA-MTX synthesized nanoplatforms clearly indicated intramolecular interactions between GO layers, HSA and MTX molecules. The absorption peaks of MTX and HSA are still observable in the UV-Vis spectrum of the formulated nanostructures upon protein and drug loading confirming the FT-IR results that strong interactions between the structure of HSA protein and MTX molecules are established onto GO-COOH surface.

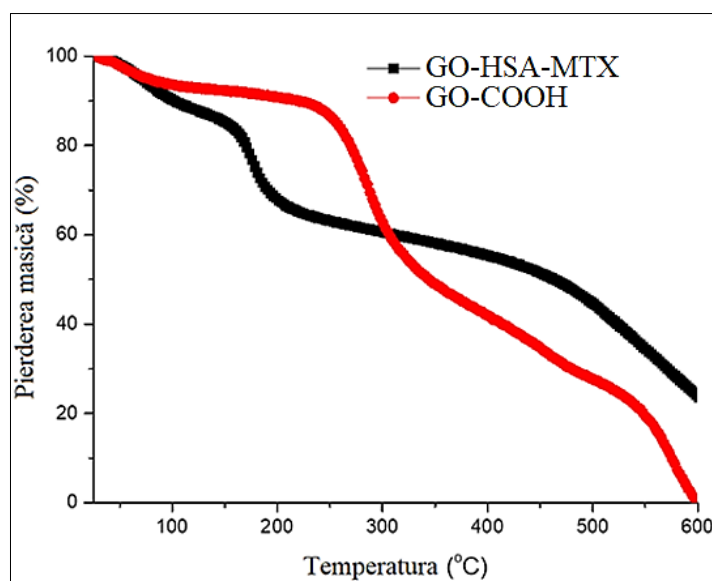


Figure 4. The TGA curves of GO-COOH and GO-HSA-MTX nanoplatforms

The developed nanoplatforms were also characterized through UV-Vis spectroscopy. As presented in Figure 5, the UV-Vis spectrum of the MTX drug shows strong π - π^* interactions at 258, 304 and 372 nm wavelengths due to the presence of heteroatomic pterine chromophore [27]. In the case of HSA protein, the UV-Vis spectrum presents only one absorption peak at 279 nm which is assigned to the presence of aromatic amino acids from the protein structure such as tryptophan, tyrosine, and phenylalanine [28, 29]. The UV-Vis spectrum of GO-HSA-MTX synthesized nanoplatforms clearly indicated intramolecular interactions between GO layers, HSA and MTX molecules. The absorption peaks of MTX and HSA are still observable in the UV-Vis spectrum of the formulated nanostructures upon protein and drug loading confirming the FT-IR results that strong interactions between the structure of HSA protein and MTX molecules are established onto GO-COOH surface.

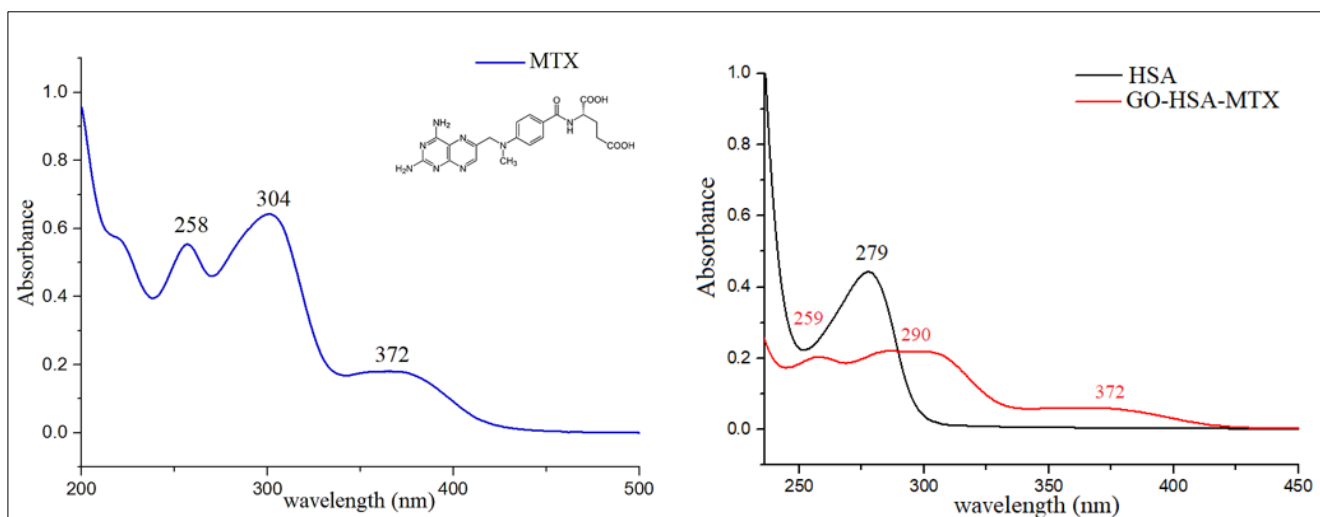


Figure 5. The UV-Vis spectra of MTX drug, HSA protein and GO-HSA-MTX nanoplateforms

The cumulative MTX drug release profiles from the GO-HSA-MTX nanoplateforms are presented in Figure 6. The *in vitro* release behavior was investigated in PBS in normal physiological environment ($pH=7.4$) and simulated tumor tissue environment ($pH=5.3$) at $37^{\circ}C$. Thus, MTX release exhibits the classic biphasic release profile, characterized by an initial burst of release of the initially encapsulated therapeutic agent, followed by a second phase in which MTX release shows a much slower and controlled release curve. In case of tumor tissue conditions simulation, in the first 30 min $\sim 35\%$ of the amount of drug encapsulated in GO-HSA-MTX is released, after 6 h the MTX concentration in the release medium increases to $\sim 43\%$, and after 24 h it reaches the value of $\sim 50\%$ and remains relatively constant until the end of the experiment (48 h). Under normal physiological conditions, the chemotherapeutic drug release from GO-HSA-MTX nanostructures is much more slowly achieved, showing that the formulated nanostructure based on GO-HSA loaded with MTX exhibits better capability to be selectively released and responsive under acidic conditions similar to the tumor microenvironments, being suitable nanoplateforms for prolonged drug release.

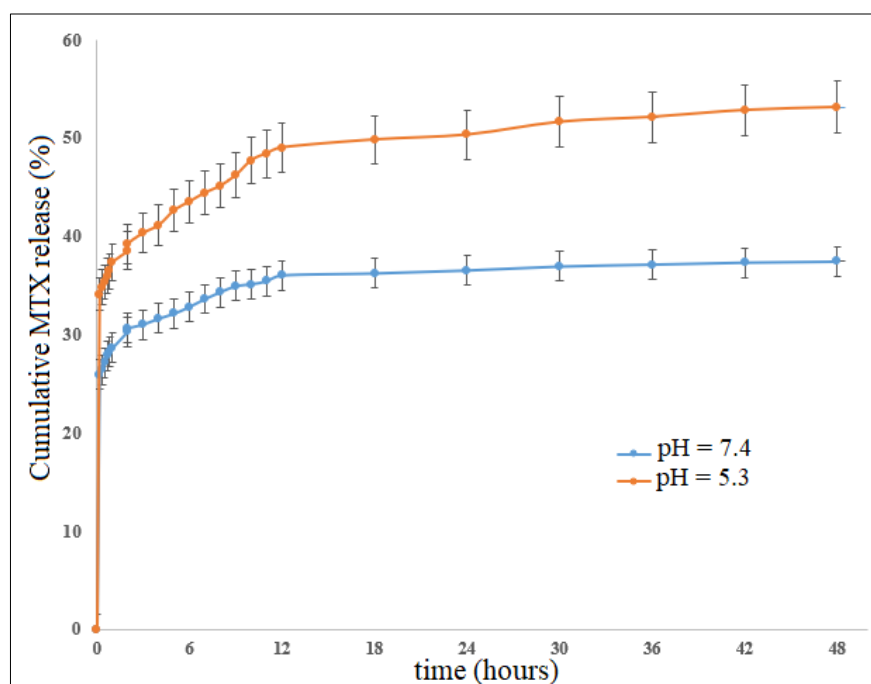


Figure 6. The cumulative *in vitro* release profiles of MTX drug from GO-HSA-MTX nanoplateforms (data are presented as mean \pm standard deviation, $n=3$)

4. Conclusions

In this study, new complex nanostructures have been developed based on covalent interactions between GO-COOH layers and HSA protein with potential applications as efficient nanoplateforms for MTX loading for drug delivery and tumor targeting. Herein, the surface of the carboxylated GO has been chemically modified with the albumin protein in order to ensure the required biocompatibility and avoid any graphene aggregates formation. Furthermore, the newly developed GO-HSA conjugates were submitted to non-covalent functionalization with MTX drug leading to formation of GO-HSA-MTX nanoplateforms capable of controlled drug release both in physiological and tumor simulated conditions. The successful functionalization of the GO-COOH layers with HSA structure and the adsorption of the MTX molecules on the surface of GO-HSA nanoplateforms were evidenced both through FT-IR and UV-Vis spectroscopy. Moreover, Raman spectrometry was employed for the structural investigation of the GO-COOH layers before and after the functionalization with HSA and MTX molecules showing a higher degree of exfoliation for the final product. Finally, the MTX release was simulated in physiological and acidic conditions in order to mimic the tumor microenvironment. Using UV-Vis spectroscopy, the drug release was monitored in time and it was observed that GO-HSA-MTX shows better capability to be selectively released under acidic conditions, being suitable nanoplateforms for pro-longed drug release. Additionally, the thermostability of the GO-HSA-MTX nanoplateforms was investigated through TGA showing that the final product presents superior thermostability compared to the raw GO-COOH structures as a result of multiple covalent interactions between the carboxylated GO layers, HSA protein and MTX molecules.

Acknowledgments: This work has been funded by the European Social Fund from the Sectoral Operational Programme Human Capital 2014-2020, through the Financial Agreement with the title "Training of PhD students and postdoctoral researchers in order to acquire applied research skills - SMART", Contract no. 13530/16.06.2022 - SMIS code: 153734.

References

1. JAO, D., XUE, Y., MEDINA, J., HU, X., Protein-Based Drug-Delivery Materials, *Materials (Basel, Switzerland)* **2017**, *10*, [doi:10.3390/ma10050517](https://doi.org/10.3390/ma10050517).
2. VOICU, A.I., GĂREA, S.A., VASILE, E., GHEBAUR, A., IOVU, H., Hybrid Hosts Based on Sodium Alginate and Porous Clay Heterostructures for Drug Encapsulation, **2021**, *13*, 2803.
3. KIANFAR, E., Protein nanoparticles in drug delivery: animal protein, plant proteins and protein cages, albumin nanoparticles, *Journal of Nanobiotechnology* **2021**, *19*, 159, [doi:10.1186/s12951-021-00896-3](https://doi.org/10.1186/s12951-021-00896-3).
4. LEE, K.Z., JEON, J., JIANG, B., SUBRAMANI, S.V., LI, J., ZHANG, F., Protein-Based Hydrogels and their Biomedical Applications, **2023**, *28*, 4988.
5. LEU ALEXA, R., IOVU, H., GHITMAN, J., SERAFIM, A., STAVARACHE, C., MARIN, M.-M., IANCHIS, R., 3D-Printed Gelatin Methacryloyl-Based Scaffolds with Potential Application in Tissue Engineering, **2021**, *13*, 727.
6. PAN, X., VERONIAINA, H., SU, N., SHA, K., JIANG, F., WU, Z., QI, X., Applications and developments of gene therapy drug delivery systems for genetic diseases, *Asian journal of pharmaceutical sciences* **2021**, *16*, 687-703, [doi:10.1016/j.ajps.2021.05.003](https://doi.org/10.1016/j.ajps.2021.05.003).
7. MIAO, Y., YANG, T., YANG, S., YANG, M., MAO, C., Protein nanoparticles directed cancer imaging and therapy, *Nano Convergence* **2022**, *9*, 2, [doi:10.1186/s40580-021-00293-4](https://doi.org/10.1186/s40580-021-00293-4).
8. KAFLE, U., AGRAWAL, S., DASH, A.K., Injectable Nano Drug Delivery Systems for the Treatment of Breast Cancer. *Pharmaceutics* **2022**, *14*, [doi:10.3390/pharmaceutics14122783](https://doi.org/10.3390/pharmaceutics14122783).
9. CHANG, J., YU, B., SALTZMAN, W.M., GIRARDI, M., Nanoparticles as a Therapeutic Delivery System for Skin Cancer Prevention and Treatment, *JID Innovations* **2023**, *3*, 100197, [doi:https://doi.org/10.1016/j.xjidi.2023.100197](https://doi.org/10.1016/j.xjidi.2023.100197).



- 10.SARKIS, M., MINASSIAN, G., MITRI, N., RAHME, K., FRACASSO, G., EL HAGE, R., GHANEM, E., D2B-Functionalized Gold Nanoparticles: Promising Vehicles for Targeted Drug Delivery to Prostate Cancer, *ACS Applied Bio Materials* **2023**, 6, 819-827, [doi:10.1021/acsabm.2c00975](https://doi.org/10.1021/acsabm.2c00975).
- 11.LARSEN, M.T., KUHLMANN, M., HVAM, M.L., HOWARD, K.A. Albumin-based drug delivery: harnessing nature to cure disease, *Molecular and cellular therapies* **2016**, 4, 3, [doi:10.1186/s40591-016-0048-8](https://doi.org/10.1186/s40591-016-0048-8).
- 12.DOCKAL, M., CARTER, D.C., RÜKER, F., Conformational transitions of the three recombinant domains of human serum albumin depending on pH, *The Journal of biological chemistry* **2000**, 275, 3042-3050, [doi:10.1074/jbc.275.5.3042](https://doi.org/10.1074/jbc.275.5.3042).
- 13.DEBNATH, S.K., SRIVASTAVA, R., Drug Delivery With Carbon-Based Nanomaterials as Versatile Nanocarriers: Progress and Prospects. **2021**, 3, [doi:10.3389/fnano.2021.644564](https://doi.org/10.3389/fnano.2021.644564).
- 14.RILEY, P.R., NARAYAN, R.J., Recent advances in carbon nanomaterials for biomedical applications: A review, *Current Opinion in Biomedical Engineering* **2021**, 17, 100262, [doi:https://doi.org/10.1016/j.cobme.2021.100262](https://doi.org/10.1016/j.cobme.2021.100262).
- 15.KHAKPOUR, E., SALEHI, S., NAGHIB, S.M., GHORBANZADEH, S., ZHANG, W., Graphene-based nanomaterials for stimuli-sensitive controlled delivery of therapeutic molecules, **2023**, 11, [doi:10.3389/fbioe.2023.1129768](https://doi.org/10.3389/fbioe.2023.1129768).
- 16.BORZOOEE MOGHADAM, N., AVATEFI, M., KARIMI, M., MAHMOUDIFARD, M., Graphene family in cancer therapy: recent progress in cancer gene/drug delivery applications, *Journal of Materials Chemistry B* **2023**, 11, 2568-2613, [doi:10.1039/D2TB01858F](https://doi.org/10.1039/D2TB01858F).
- 17.SHAFIEE, A., IRAVANI, S., VARMA, R.S., Graphene and graphene oxide with anticancer applications: Challenges and future perspectives, *MedComm* **2022**, 3, e118, [doi:10.1002/mco2.118](https://doi.org/10.1002/mco2.118).
- 18.JAFARI, A., KHANMOHAMMADI CHENAB, K., MALEKTAJ, H., FARSHCHI, F., GHORBANI, S., GHASEMIAMINEH, A., KHOSHAKHLAGH, M., ASHTARI, B., ZAMANI-MEYMIAN, M.-R., An attempt of stimuli-responsive drug delivery of graphene-based nanomaterial through biological obstacles of tumor, *FlatChem* **2022**, 34, 100381, [doi:https://doi.org/10.1016/j.flatc.2022.100381](https://doi.org/10.1016/j.flatc.2022.100381).
- 19.QUAGLIARINI, E., POZZI, D., CARDARELLI, F., CARACCIOLO, G., The influence of protein corona on Graphene Oxide: implications for biomedical theranostics, *Journal of Nanobiotechnology* **2023**, 21, 267, [doi:10.1186/s12951-023-02030-x](https://doi.org/10.1186/s12951-023-02030-x).
- 20.LIU, H., JIANG, Y., WANG, Z., ZHAO, L., YIN, Q., LIU, M., Nanomaterials as carriers to improve the photodynamic antibacterial therapy, *Frontiers in chemistry* **2022**, 10, 1044627, [doi:10.3389/fchem.2022.1044627](https://doi.org/10.3389/fchem.2022.1044627).
- 21.GUO, S., SONG, Z., JI, D.K., REINA, G., FAUNY, J.D., NISHINA, Y., MÉNARD-MOYON, C., BIANCO, A., Combined Photothermal and Photodynamic Therapy for Cancer Treatment Using a Multifunctional Graphene Oxide, *Pharmaceutics* **2022**, 14, [doi:10.3390/pharmaceutics14071365](https://doi.org/10.3390/pharmaceutics14071365).
- 22.SONTAKKE, A.D., TIWARI, S., PURKAIT, M.K., A comprehensive review on graphene oxide-based nanocarriers: Synthesis, functionalization and biomedical applications, *FlatChem* **2023**, 38, 100484, [doi:https://doi.org/10.1016/j.flatc.2023.100484](https://doi.org/10.1016/j.flatc.2023.100484).
- 23.USOLTSEV, D., SITNIKOVA, V., KAJAVA, A., USPENSKAYA, M., Systematic FTIR Spectroscopy Study of the Secondary Structure Changes in Human Serum Albumin under Various Denaturation Conditions, *Biomolecules* **2019**, 9, [doi:10.3390/biom9080359](https://doi.org/10.3390/biom9080359).
- 24.WOJTONISZAK, M., URBAS, K., PERUŻYŃSKA, M., KURZAWSKI, M., DROŹDZIK, M., MIJOWSKA, E., Covalent conjugation of graphene oxide with methotrexate and its antitumor activity, *Chemical Physics Letters* **2013**, 568-569, 151-156, [doi:https://doi.org/10.1016/j.cplett.2013.03.050](https://doi.org/10.1016/j.cplett.2013.03.050).
- 25.FERRARI, A.C., BASKO, D.M., Raman spectroscopy as a versatile tool for studying the properties of graphene, *Nature Nanotechnology* **2013**, 8, 235-246, [doi:10.1038/nnano.2013.46](https://doi.org/10.1038/nnano.2013.46).



26. BARJOLA, A., TORMO-MAS, M.Á., SAHUQUILLO, O., BERNABÉ-QUISPE, P., PÉREZ, J.M., GIMÉNEZ, E., Enhanced Antibacterial Activity through Silver Nanoparticles Deposited onto Carboxylated Graphene Oxide Surface. **2022**, *12*, 1949.
27. AYYAPPAN, S., SUNDARAGANESAN, N., AROULMOJI, V., MURANO, E., SEBASTIAN, S., Molecular structure, vibrational spectra and DFT molecular orbital calculations (TD-DFT and NMR) of the antiproliferative drug Methotrexate. *Spectrochimica Acta Part A: Molecular and Biomolecular Spectroscopy* **2010**, *77*, 264-275, doi:<https://doi.org/10.1016/j.saa.2010.05.021>.
28. PANJA, S., KHATUA, D.K., HALDER, M., Simultaneous Binding of Folic Acid and Methotrexate to Human Serum Albumin: Insights into the Structural Changes of Protein and the Location and Competitive Displacement of Drugs. *ACS Omega* **2018**, *3*, 246-253, doi:10.1021/acsomega.7b01437.
29. BAIG, M.H., RAHMAN, S., RABBANI, G., IMRAN, M., AHMAD, K., CHOI, I., Multi-Spectroscopic Characterization of Human Serum Albumin Binding with Cyclobenzaprine Hydrochloride: Insights from Biophysical and In Silico Approaches. *International journal of molecular sciences* **2019**, *20*, doi:10.3390/ijms20030662.

Manuscript received: 13.10.2023